HHS Public Access

Author manuscript

Mol Cell Pharmacol. Author manuscript; available in PMC 2015 April 15.

Published in final edited form as:

Mol Cell Pharmacol. ; 6(2): 15–25.

Tenfibgen-DMAT Nanocapsule Delivers CK2 Inhibitor DMAT to Prostate Cancer Xenograft Tumors Causing Inhibition of Cell Proliferation

Janeen H. Trembley[1,3,5], **Gretchen M. Unger**[6], **Omar Cespedes Gomez**[1,3], **Md. J. Abedin**[1,3], **Vicci L. Korman**[6], **Rachel I. Vogel**[5], **Gloria Niehans**[2], **Betsy T. Kren**[1,5], and **Khalil Ahmed**[1,3,4,5]

[1]Research Service, Minneapolis VA Health Care System, Minneapolis

[2]Pathology and Laboratory Medicine Service, Minneapolis VA Health Care System, Minneapolis

[3]Department of Laboratory Medicine and Pathology, University of Minnesota, Minneapolis

[4]Department of Urology, University of Minnesota, Minneapolis

[5]Masonic Cancer Center, University of Minnesota, Minneapolis

[6]GeneSegues Inc., Chaska, Minnesota

Abstract

CK2 is a master regulator protein kinase which demonstrates heightened expression in diverse cancer types and is considered a promising target for therapy. Given its ubiquitous expression and potent influence on cell survival, cancer cell-directed targeting of the CK2 signal is an important factor for development of an anti-CK2 therapeutic. We previously reported on the malignant cell specificity and effect on CK2 signaling of a tenfibgen (TBG) based nanocapsule for delivery of the CK2 small molecule inhibitor 2-dimethylamino-4,5,6,7-tetrabromo-1*H*-benzimidazole (DMAT) in cultured prostate cancer cells. Here we tested the ability of TBG-DMAT to affect the growth of prostate xenograft tumors in mice. Our results show that treatment of PC3-LN4 xenograft tumors with TBG-DMAT caused loss of proliferative Ki-67 signal as well as Nuclear Factor-kappa B (NF-κB) expression in the tumors. Further, the TBG-DMAT nanocapsule was detected in tumors and not in liver or testis. In conclusion, TBG-based nanocapsule delivery of anti-CK2 small molecule drugs holds significant promise for treatment of prostate cancer.

Correspondence: Janeen H. Trembley, Cellular and Molecular Biochemistry Research Laboratory (151), Minneapolis VA Health Care System, One Veterans Drive, Minneapolis, MN 55417, USA. trem0005@umn.edu. Khalil Ahmed, Cellular and Molecular Biochemistry Research Laboratory (151), Minneapolis VA Health Care System, One Veterans Drive, Minneapolis, MN 55417, USA. Tel. 612-467-2594. ahmedk@umn.edu.

Disclaimer: The views expressed in this article are those of the authors and do not necessarily reflect the position or policy of the U.S. Department of Veterans Affairs or the U.S. government.

Conflicts of Interest

GMU has ownership interest (including patents) in GeneSegues, Inc. No potential conflicts of interest were disclosed by the other authors.

Keywords

CK2; Prostate Cancer; Nanocapsule; Nanoparticle; DMAT; Tenfibgen

Introduction

CK2 (formerly casein kinase II or CKII) is a ubiquitous Ser/Thr protein kinase with a heterotetrameric structure in which two catalytic subunits (42 kDa α and/or 38 kDa α′) are linked together by two regulatory subunits (28 kDa β) into $\alpha_2\beta_2$, $\alpha\alpha'\beta_2$, or $\alpha'_2\beta_2$ configurations. This kinase has been found associated with various cellular compartments and organelles, including chromatin, matrix and nucleoli within the nuclei, and endoplasmic reticulum, Golgi, mitochondria and cytoskeleton within the cytoplasm (1). In keeping with the diverse cellular locations, CK2 phosphorylation of its numerous substrates influences cellular functions on myriad levels – many of which impact cancer-related signaling (2). Importantly, CK2 is essential for survival (3–6). Although mutational changes in CK2 genes are not generally observed, increased CK2 expression and activity is very consistently detected across the spectrum of diverse cancers (7–9). Additionally, although aspects of regulation continue to emerge which modulate CK2 activity, overall CK2 exhibits constitutive activity in cells and does not require specific activation (6, 10–12). Taken in sum, CK2 is undoubtedly an important contributor to the cancer phenotype, making it an attractive target for anti-cancer therapeutic development (13).

CK2 steady-state expression levels in normal cells under quiescent conditions are generally very stable. However, the increased CK2 levels observed in all cancers have led to the descriptor of CK2 as a “nononcogene” (8, 9, 14). As such, CK2 expression functions to maintain the many activities sustaining cancer cell growth and survival. CK2 elevated steady-state protein and, more rarely, RNA expression levels as well as altered intracellular distribution favoring nuclear localization reflects both the dysplastic as well as proliferative status of neoplastic cells (7, 8, 15). Moreover, these expression characteristics correlate with disease severity and prognosis (15–22). Finally, the ever increasing documentation for CK2 roles in protecting cells from cell death reinforces the connection between CK2 upregulation and the cancer cell phenotype (9, 23–24).

Anti-cancer targeting of CK2 can be accomplished via multiple avenues. Protein expression can be blocked using oligonucleotides to promote cleavage and degradation or hinder translation of the RNA transcript. Alternately, protein catalytic activity can be quashed using small molecule chemical inhibitors as well as peptide inhibitors. Numerous CK2 small molecule inhibitors exist and continue to be developed (25). These CK2 inhibitors cause loss of cell viability and induce cell death in cultured cells (26–36). Further, CK2 small molecule inhibitors have been employed to assess their effects in animal models of cancer and retinal neovascularization (36–42).

Irrespective of the androgen receptor status, inhibition or down regulation of CK2 is effective for killing prostate cancer cells (13, 43, 44). Regardless of the therapeutic approach used, an important aspect to consider when targeting CK2 is the essential and ubiquitous nature of the signal. Administration of a CK2-targeted drug in a vehicle designed to

specifically enter malignant but not normal cells would be advantageous for systemic delivery. The drug delivery barriers of bioavailability, *in vivo* protection of the cargo, and specific targeting to tumor cells are surmounted by our nanocapsule technology (45). This nanocapsule is designed to form a sub-50 nanometer size (s50) particle composed of a protein ligand (tenfibgen or TBG) (46) shell completely enclosing the cargo thus providing both receptor targeting and protection of the drug (44, 47–48).

Previously, we reported that the TBG nanoencapsulated anti-CK2 small molecule inhibitor DMAT (TBG-DMAT) as well as TBG nanoencapsulated siRNA directed against both catalytic subunits of CK2 potently affected the proliferation and viability of cultured malignant but not benign prostate cells (44). We have further demonstrated that delivery of a single stranded anti-CK2 oligonucleotide effectively reduces both primary and metastatic tumors in prostate and in head and neck squamous cell cancers (48, 49). Here, we have expanded this work in a small animal study to investigate the effects of a TBG nanoencapsulated chemical inhibitor of CK2 (DMAT) on human prostate cancer xenograft tumors in nude mice. Our results indicate that TBG-DMAT enters the cancer cells *in vivo* and affects the proliferation and signaling in the xenograft tumor suggesting the feasibility of utilizing TBG nanoencapsulated small molecule drugs for cancer cell-specific therapeutic targeting of CK2.

Material and Methods

Cell Lines

PC3-LN4 cells, obtained as previously described (50), were maintained in monolayer culture containing RPMI 1640 supplemented with 10% fetal bovine serum (FBS), 2 mM L-glutamine, and penicillin-streptomycin (51). Cells had undetectable levels of mycoplasma, and this cell line was authenticated by the Genetics Resources Core Facility at Johns Hopkins University.

Reagents

Antibodies used were: CK2α and CK2α′ (Bethyl Laboratories A300-197A and A300-199A), CK2β (Santa Cruz sc-46666), actin (Santa Cruz sc-1616), p-NF-κB p65 Ser 529 (Santa Cruz sc-101751), NF-κB p65 (BD Transduction Laboratories 610869), caspase 3 and cleaved caspase 3 (Cell Signaling 9662 & 9661). The 2-dimethylamino-4,5,6,7-tetrabromo-1*H*-benzimidazole (DMAT, compound 2c), a generous gift from L.A. Pinna, was synthesized as described previously (52); it was suspended in DMSO (HybriMax, Sigma) at a concentration of 5 mg/ml and filtered 0.1 μm (6809-7013, Whatman) using an extruder prior to use. Aliquots for use as naked DMAT in mice were flash frozen in liquid nitrogen and stored at −80 °C.

Animals

Male athymic NCr nude (Nu/Nu) mice (01B74, National Cancer Institute) were maintained under pathogen-free conditions. PC3-LN4 tumors were initiated by subcutaneous injection of 2×10^6 cells in 50% matrigel (354234, BD Biosciences) in the mouse flank when mice were approximately eight weeks old. The animal facilities were approved by the Association

for Assessment and Accreditation of Laboratory Animal Care International in accordance with the current regulations and standards of the USDA, U.S. Department of Health and Human Services, and NIH. Animal experiments were conducted in the Minneapolis VA Health Care System animal facility in accordance with an approved IACUC protocol.

In vivo Therapy of Xenograft Human Prostate Cancer in Athymic Nude Mice

Therapy was initiated when tumors reached an average size of 150 – 300 mm^3 calculated by the formula V = (L × W × W)/2. Lyophilized TBG-DMAT aliquots were resuspended by rocking in sterile water for 1 h and sterile filtered (0.2 μm, 09-720-3, Fisher Scientific) before use in mice. For one group of mice, TBG-DMAT (100 μg/kg, in 10% lactitol/PBS (w/v)) was administered once daily, 2 doses given iv, then 6 doses given ip (total of 8 doses over 8 days). A second group was given TBG-DMAT administered once daily, 2 doses given iv at 100 μg/kg, then 4 doses given ip at 20 μg/kg (total of 6 doses over 6 days). This group is referred to as the 20 μg/kg group. In a third group, naked (i.e., non-encapsulated) DMAT was administered once daily ip at a dose of 500 μg/kg over 6 days. In this case, the 5 mg/ml DMAT in DMSO stock solution was diluted into 10% lactitol/PBS just prior to injection. A fourth group of mice was given a daily injection of vehicle (10% lactitol/PBS) over 8 days. Mice were sacrificed 1 day after the final treatment, the PC3-LN4 flank tumors were excised, weighed, sliced in half for removal of liquefied dead tissue material, weighed again, and processed for formalin fixation or snap frozen in liquid nitrogen for further analysis.

Immunoblot Analysis of DMAT Treated Tumors

Approximately 0.1 g of frozen tumor tissue was minced and homogenized in 1 ml of CSK buffer (53). One ninth volume of 10× RIPA buffer (53) was added to the homogenate and the lysate incubated on ice for 30 min with pipet mixing every 10 min. The lysate was centrifuged (17,000 × g) at 4 °C for 10 min. The resulting supernatant was quantitated using the Bradford assay (Thermo Scientific 23238), and 40 μg of each lysate was separated using the NuPAGE 4–12% Bis-Tris Midi gel system (Life Technologies)and subjected to immunoblot analysis (53).

Immunofluorescence Analysis for Syrian Hamster IgG

Detection of Syrian hamster IgG $F(ab)_2$ fragment (incorporated into the TBG-DMAT nanocapsule) release within tumor, liver and testis tissues was performed as described (48).

Ki-67 and H&E Staining of Tumors

Immunostaining for Ki-67 and H&E was performed by the Pathology and Laboratory Medicine Service (Minneapolis VA Health Care System). Analysis of the Ki-67 staining was performed using the ImmunoRatio web application (54). Analysis of the H&E stained liver and testis sections was performed by visual microscopic inspection by a pathologist of 6 sections per tissue per mouse.

Nanocapsule Preparation

TBG nanocapsules were prepared and characterized as previously described (44). The nanocapsule preparation was concentrated by centrifugation (VivaSpin 20, Sartorius), divided into aliquots, lyophilized, and stored at −80 °C. The yield of DMAT incorporation in the nanocapsule was 0.24% as determined by neutron activation analysis based on the 4 Br residues in DMAT so that ^{80}Br was produced by neutron capture reaction from ^{79}Br which allowed for the quantitation of DMAT in the nanocapsule. The general characteristics of s50 TBG-DMAT are shown in Table 1.

Statistical Analysis

Percent dead tumor and immunoblot expression data were compared by treatment group using analysis of variance (ANOVA) methods. The percent Ki-67 positive cells was compared by treatment using ANOVA methods, additionally adjusting for repeated measures within mice. Final tumor weight following treatment was compared by group using ANOVA, adjusting for baseline tumor weight. Means ± standard errors (SE) are presented unless otherwise noted. P-values for pair wise comparisons and comparisons with the control group, as appropriate, were adjusted for multiple comparisons using Bonferroni correction and Dunnett's methods, respectively. P-values <0.05 were considered statistically significant.

Results

Effect of TBG-DMAT compared with naked DMAT on prostate cancer xenograft tumors

We have previously documented that a comparison of naked (unformulated) DMAT and s50 TBG encapsulated DMAT showed a clear distinction in targeting CK2 in cultured prostate cancer cells. Both benign prostate cells (BPH-1) and prostate cancer cells responded to naked DMAT; however, only cancer cells responded to TBG-DMAT treatment. These results were concordant for measures of cell growth and analyses of CK2 activity responsive targets (44). We therefore decided to compare the effects of unformulated DMAT and TBG-DMAT on PC3-LN4 human prostate cancer xenograft tumors in mice. The TBG-DMAT nanocapsules were formulated as slightly negative, single, uniform nanocapsules with an average elliptical diameter of 14.6 nm (Table 1). A representative transmission electron microscopy image is shown in Figure 1.

Systemic treatment was initiated when flank tumors reached 150 – 300 mm^3 in size, designated as day 1. Three treatment groups and one control group were set up. The TBG-DMAT 100 μg/kg and vehicle control groups received daily injections for 8 days and were sacrificed on day 9. The TBG-DMAT 20 μg/kg and naked DMAT 500 μg/kg groups received daily injections for 6 days and were sacrificed on day 7. The results in Figure 2A show that TBG-DMAT at a dose of 100 μg/kg (800 μg/kg cumulative dose) produced an effect on inducing tumor cell death that was analogous to that produced by naked DMAT at 500 μg/kg dose (3000 μg/kg cumulative dose). This result suggested that the nanoencapsulated drug was more effectively available to the tumor cells compared with the unformulated drug. The efficacy of the TBG-DMAT was further indicated by the observation that its effect on tumor cells was also apparent at the lower dose of 20 μg/kg

(280 μg/kg cumulative dose, see Materials and Methods for details). Representative H&E pictures of tumors are shown in Figure 2B.

Ki-67 analysis of xenograft tumors treated with TBG-DMAT

Immunohistochemical analysis of the proliferation marker Ki-67 was performed on the tumors and representative pictures are shown in Figure 3A. Treatment using 20 or 100 μg/kg TBG-DMAT had an effect similar to that observed using 500 μg/kg naked DMAT in causing a significant reduction in Ki-67 signal. The quantitation of the immunohistochemical data is shown in Figure 3B which indicates that there was a decrease in Ki-67 positive cells compared to vehicle control cells of 20.6, 22.7, and 29.6% in the presence of 20 μg/kg TBG-DMAT ($p=0.002$), 100 μg/kg TBG-DMAT ($p=0.001$), and 500 μg/kg DMAT ($p=0.001$), respectively. These results are consistent with those for tumor tissue death under these conditions shown in Figure 2.

We performed immunohistochemical TUNEL analysis as well as immunofluorescence analysis for blood vessel markers (MECA-32, CD31, CD105) in these tumors, but no statistically significant differences were detected (data not shown).

Immunoblot analysis of xenograft tumors treated with TBG-DMAT

Analysis of the whole cell lysates of tumor tissues was undertaken to determine the molecular response to CK2 inhibition. The results in Figure 4 show the immunoblots for the various CK2 subunits and NF-κB p65 in tumor lysates from treatment with TBG-DMAT and DMAT as described under Figure 1 and quantified data are presented in Table 2. The results are shown for each mouse in the various treatment groups. No change in the CK2 signal for the α, α′ or β subunits was noted in tumors treated with 100 μg/kg TBG-DMAT or 500 μg/kg DMAT; however, a reduction in the CK2α and α′ signals was detected at the 20 μg/kg TBG-DMAT treatment dose ($p=0.004$ and $p=0.0004$, respectively). The data demonstrated no detectable change in full length caspase 3 as well as no detection of cleaved caspase 3 in response to the various treatments (data not shown). In contrast to our results using cultured cells, under these experimental conditions we did not notice a remarkable response in the CK2-mediated phosphorylation of NF-κB p65 at Ser 529 (44). However, the overall amount of immunoreactive NF-κB p65 protein was found to be significantly reduced in the presence of DMAT treatment, particularly at 20 μg/kg ($p=0.023$).

Analysis of pathological effects and drug biodistribution in animals treated with TBG-DMAT

The animals subjected to TBG-DMAT therapy were evaluated for any effect on their body weight. The treatment regimen did not show any significant effect on mouse total body weight (Figure 5A). The biggest change was observed in the vehicle treated animals in which a decrease in body weight of 5.4% was observed. The TBG-DMAT nanocapsules contained the $F(ab')_2$ fragment of Syrian hamster IgG within the TBG protein coat, which was used as a marker for identification of the nanocapsule within tissues. The presence of TBG-DMAT in tumor, liver and testis was evaluated in formalin fixed and paraffin embedded sections by indirect immunofluorescence analysis for Syrian hamster IgG. The results shown in Figure 5B demonstrated that cytosolic Syrian hamster IgG signal was

detected in TBG-DMAT treated tumors 24 hours after the final treatment. No nanocapsule signal was detected in the liver or testis from the same TBG-DMAT treated mice (Figure 5B, upper right panels). The images captured from the tumors, liver and testes of naked DMAT treated mice served as background controls (Figure 5B, lower panels). Finally, hematoxylin and eosin stained sections from liver and testis of each mouse in the study were evaluated for any effect on their pathology. As illustrated in Figure 5C, the liver and testis from these animals revealed no damage as a consequence of the daily therapy with TBG-DMAT.

DISCUSSION

The unique potential of targeting CK2 for cancer therapy has gained widespread acceptance since we described the original utility of anti-CK2 treatment in 2001 (13, 55). A considerable effort is directed at evaluating CK2 small molecule inhibitors for targeting CK2. However, though a small pharmacological window for targeting of CK2 may exist (36, 50, 56), we believe it an essential component of design to target CK2 in a cancer specific manner (13). This belief is germane because CK2 is a ubiquitously expressed and essential cell survival signal, and thus its loss in normal cells could induce host toxicity. To that end, we have previously reported on the utility of our novel delivery system to target CK2 in cancer cells and not the normal cells. Here we have examined the potential of delivering the CK2 inhibitor DMAT in TBG nanocapsule format to target the enzyme in a cancer specific manner to complement our observation of TBG-DMAT effects on cultured cells. The model we chose for these studies, PC3-LN4, represents PTEN-null, androgen receptor (AR) non-expressing, androgen-independent metastatic prostate cancer; although it has been shown that AR expression can be restored in PC3 cells (51, 57). Current views in the field typically argue that, despite castration resistance, AR signaling is important to prostate cancer cell survival (58, 59). However, there is also evidence for androgen independent and AR expression-negative roles in CRPC development, including PTEN null cancers (60–63). Thus, the use of models in which AR expression is not detectable and the cells are androgen-independent has relevance for therapeutic studies.

The nanocapsule shell employed here was constructed of tenfibgen (TBG). TBG is the C-terminal fibrinogen globe domain of the 225 kDa fibronectin-like extracellular matrix protein tenascin-C (TN-C) that is prominent in specialized embryonic tissues, wound healing, and tumors (46). With the exception of wound healing, normal adult cells do not migrate on tenascin (64, 65). Similar to many other cancer types, stroma rich in TN-C is observed adjacent to areas of prostate cancer cells (66, 67). TN-C expression is also connected with the vascularization and metastatic activity of tumors (68–70). The TBG domain of TN-C demonstrates angiogenic behavior and contains a binding site for receptors such as $\alpha v\beta 3$ integrin (71). These TN-C/TBG cell receptors are elevated in the caveoli of cancer cells, whereas they are typically minimal in normal cells (66, 72). In a previous report, we showed that the TBG nanocapsule facilitated the delivery of both siRNA and DMAT to cultured cells and produced appropriate effects on CK2 activity or expression specifically in malignant but not benign cells (44).

In developing the TBG-DMAT nanocapsule, we observed that the incorporation of DMAT in the TBG nanocapsule was significantly lower than that observed by our group for encapsulation of nucleic acid molecules. For example, the relative yield of DMAT encapsulation here was 0.24% compared with greater than 78% encapsulation of antisense- or siRNA-CK2 we previously reported (44, 48). As a result, in the present study we were limited in the dose level of DMAT as well as duration of dosing that could be delivered *in vivo*. However, despite the observed limitation of DMAT incorporation in the nanocapsule affecting the amount of drug deliverable *in vivo*, we investigated the effectiveness of TBG-DMAT compared with unformulated DMAT in targeting CK2 and inducing cell death in xenograft tumors *in vivo*.

The resulting observations indicate several important points. First, our data provide evidence that TBG-DMAT induces loss of tumor cell proliferation *in vivo* at a much lower concentration of DMAT than when it is delivered as naked DMAT. Second, the duration of the treatment with TBG-DMAT nanocapsules did not produce any toxicity or organ damage in the mouse as evidenced by a lack of any change in the liver and testis histology or in the animal body weight. One unexpected observation was the reduced expression of CK2α and CK2α′ proteins in the 20 μg/kg TBG-DMAT treatment group. A recent report demonstrated that CK2 kinase activity indirectly impacts expression from CK2α and CK2β gene promoter constructs, and transcription from the reporter constructs was attenuated after CK2 inhibition (73). Thus one explanation for decreased CK2αα′ protein levels is a feedback mechanism on CK2 gene expression after DMAT inhibition of CK2 activity. Further, it has been observed that certain drugs elicit differing effects within a system depending on the dose level, in which the lower doses give one result compared to that observed using a higher dose, and where both dose levels may be considered effective depending on the desired or measured outcome (74). We do not have sufficient data using the TBG-DMAT therapeutic to conclude that such a response is occurring here with respect to degree of CK2 inhibition and its effect on CK2 gene expression, but put forth the possibility that something of this nature could explain the differing effects of 100 versus 20 μg/kg doses on CK2 expression. Regardless of the effect on CK2 protein expression, both doses caused a significant loss of proliferation. While molecular and biochemical evidence of the CK2 targeting was apparent, we could not study the effect of higher concentrations or more prolonged use of the drug. Nonetheless, we surmise that if a more prolonged treatment of DMAT could be delivered via the TBG-DMAT nanocapsules, this could result in a more robust response to this CK2 targeting cancer cell-specific therapeutic approach.

The potential significance of our observations is pertinent in light of the previous *in vivo* studies undertaken with DMAT and other CK2 inhibitors for their possible utility as cancer therapeutics. For example, oral administration of CX-4945, an ATP-competitive inhibitor of CK2, inhibited growth of a number of xenograft cancers in mice (36, 40, 75) In another report, reduced growth in hepatocellular carcinoma xenograft tumors after treatment with DMAT was observed in conjunction with interference with NK-κB activation and Wnt signaling (39). Other work on developing novel inhibitors of CK2 for cancer therapy suggests their potential application to therapeutic targeting (76). Yet, the concern of affecting normal cells on prolonged use of such inhibitors remains. Importantly, our work

provides proof-of-concept that if small molecule CK2 inhibitors could be formulated with greater efficiency in the TBG nanoencapsulation process, there would be great utility of these drugs for elimination of tumor in a targeted manner with a minimal potential of host toxicity.

In summary, we are the first to report nanoencapsulation of a small molecule inhibitor against CK2 to specifically reduce xenograft tumor proliferation *in vivo* without affecting the benign cells. While there is a need to improve DMAT incorporation in the TBG-DMAT nanocapsule, several important features relating to targeting CK2 for cancer therapy by this approach are noteworthy. The ability of the nanocapsule drug delivery utilized by us (i.e., s50 TBG-DMAT) to specifically target cancer cells avoiding the normal cells and to deliver the drug in a protected manner without concerns relating to drug inactivation in circulation is particularly significant. Thus, our observations provide further support of the strategy that TBG nanoencapsulation technology is highly promising for cancer cell-directed treatment of malignancy.

Acknowledgments

TEM images were acquired by Richard An (IHC World, Bethesda, MD). This work is supported in part by merit review research funds (1IO1B001731) awarded by the Department of Veterans Affairs (KA), research grant CA150182 awarded by NCI, NIH, Department of Health and Human Services (KA), research grants CA158730 and DK067436-05 awarded by NCI and National Institute of Diabetes and Digestive and Kidney Diseases (NIDDK), respectively, NIH, Department of Health and Human Services (BTK), and research grants HHS-N261-2008-00027/N42CM-2008-00027C, CA99366, and CA119556 awarded by NCI, NIH, Department of Health and Human Services (GMU).

Abbreviations

AFM	atomic force microscopy
CK2	official acronym for former casein kinase 2 or II
d	day(s)
DMAT	2-dimethylamino-4,5,6,7-tetrabromo-1*H*-benzimidazole
h	hour(s)
DLS	dynamic light scattering
FBS	fetal bovine serum
ip	intraperitoneal
iv	intravenous
IHC	immunohistochemical or immunohistochemistry
kDa	kiloDalton
min	minutes
NF-κB	Nuclear Factor-kappaB
PBS	phosphate buffered saline

PCa	prostate cancer
PCR	polymerase chain reaction
P-Ser529	phosphorylated at serine residue 529
sc	subcutaneous
Ser	serine
TBG	tenfibgen
TN-C	tenascin-C

References

1. Faust M, Montenarh M. Subcellular localization of protein kinase CK2. A key to its function? Cell Tissue Res. 2000; 301:329–40. [PubMed: 10994779]
2. Filhol O, Cochet C. Protein kinase CK2 in health and disease: Cellular functions of protein kinase CK2: a dynamic affair. Cell Mol Life Sci. 2009; 66:1830–9. [PubMed: 19387551]
3. Padmanabha R, Chen-Wu JL, Hanna DE, Glover CV. Isolation, sequencing, and disruption of the yeast CKA2 gene: casein kinase II is essential for viability in Saccharomyces cerevisiae. Mol Cell Biol. 1990; 10:4089–99. [PubMed: 2196445]
4. Buchou T, Vernet M, Blond O, et al. Disruption of the regulatory β subunit of protein kinase CK2 in mice leads to a cell-autonomous defect and early embryonic lethality. Mol Cell Biol. 2003; 23:908–15. [PubMed: 12529396]
5. Seldin DC, Lou DY, Toselli P, Landesman-Bollag E, Dominguez I. Gene targeting of CK2 catalytic subunits. Mol Cell Biochem. 2008; 316:141–7. [PubMed: 18594950]
6. Trembley JH, Wang G, Unger G, Slaton J, Ahmed K. Protein kinase CK2 in health and disease: CK2: a key player in cancer biology. Cell Mol Life Sci. 2009; 66:1858–67. [PubMed: 19387548]
7. Trembley JH, Chen Z, Unger G, et al. Emergence of protein kinase CK2 as a key target in cancer therapy. BioFactors. 2010; 36:187–95. [PubMed: 20533398]
8. Ruzzene M, Pinna LA. Addiction to protein kinase CK2: a common denominator of diverse cancer cells? Biochim Biophys Acta. 2010; 1804:499–504. [PubMed: 19665589]
9. Tawfic S, Yu S, Wang H, Faust R, Davis A, Ahmed K. Protein kinase CK2 signal in neoplasia. Histol Histopathol. 2001; 16:573–82. [PubMed: 11332713]
10. Niefind K, Issinger OG. Conformational plasticity of the catalytic subunit of protein kinase CK2 and its consequences for regulation and drug design. Biochim Biophys Acta. 2010; 1804:484–92. [PubMed: 19796713]
11. Nguyen le XT, Mitchell BS. Akt activation enhances ribosomal RNA synthesis through casein kinase II and TIF-IA. Proc Natl Acad Sci U S A. 2013; 110:20681–6. [PubMed: 24297901]
12. Tarrant MK, Rho HS, Xie Z, et al. Regulation of CK2 by phosphorylation and O-GlcNAcylation revealed by semisynthesis. Nat Chem Biol. 2012; 8:262–9. [PubMed: 22267120]
13. Wang H, Davis A, Yu S, Ahmed K. Response of cancer cells to molecular interruption of the CK2 signal. Mol Cell Biochem. 2001; 227:167–74. [PubMed: 11827168]
14. Luo J, Solimini NL, Elledge SJ. Principles of cancer therapy: oncogene and nononcogene addiction. Cell. 2009; 136:823–37. [PubMed: 19269363]
15. Faust RA, Gapany M, Tristani P, Davis A, Adams GL, Ahmed K. Elevated protein kinase CK2 activity in chromatin of head and neck tumors: association with malignant transformation. Cancer Lett. 1996; 101:31–5. [PubMed: 8625279]
16. O-charoenrat P, Rusch V, Talbot SG, et al. Casein kinase II alpha subunit and C1-inhibitor are independent predictors of outcome in patients with squamous cell carcinoma of the lung. Clin Cancer Res. 2004; 10:5792–803. [PubMed: 15355908]

17. Faust RA, Niehans G, Gapany M, et al. Subcellular immunolocalization of protein kinase CK2 in normal and carcinoma cells. Int J Biochem Cell Biol. 1999; 31:941–9. [PubMed: 10533285]
18. Gapany M, Faust RA, Tawfic S, Davis A, Adams GL, Ahmed K. Association of elevated protein kinase CK2 activity with aggressive behavior of squamous cell carcinoma of the head and neck. Mol Med. 1995; 1:659–66. [PubMed: 8529132]
19. Laramas M, Pasquier D, Filhol O, Ringeisen F, Descotes JL, Cochet C. Nuclear localization of protein kinase CK2 catalytic subunit (CK2α) is associated with poor prognostic factors in human prostate cancer. Eur J Cancer. 2007; 43:928–34. [PubMed: 17267203]
20. Kim JS, Eom JI, Cheong J-W, et al. Protein Kinase CK2α as an Unfavorable Prognostic Marker and Novel Therapeutic Target in Acute Myeloid Leukemia. Clin Cancer Res. 2007; 13:1019–28. [PubMed: 17289898]
21. Lin KY, Fang CL, Chen Y, et al. Overexpression of nuclear protein kinase CK2 Beta subunit and prognosis in human gastric carcinoma. Annals Surg Oncol. 2010; 17:1695–702.
22. Lin KY, Tai C, Hsu JC, et al. Overexpression of Nuclear Protein Kinase CK2 alpha Catalytic Subunit (CK2alpha) as a Poor Prognosticator in Human Colorectal Cancer. PLoS One. 2011; 6:e17193. [PubMed: 21359197]
23. Ahmed K, Gerber DA, Cochet C. Joining the cell survival squad: an emerging role for protein kinase CK2. Trends Cell Biol. 2002; 12:226–30. [PubMed: 12062170]
24. Guo C, Yu S, Davis AT, Wang H, Green JE, Ahmed K. A potential role of nuclear matrix-associated protein kinase CK2 in protection against drug-induced apoptosis in cancer cells. J Biol Chem. 2001; 276:5992–9. [PubMed: 11069898]
25. Cozza G, Pinna LA, Moro S. Kinase CK2 inhibition: an update. Curr Med Chem. 2013; 20:671–93. [PubMed: 23210774]
26. Zhu D, Hensel J, Hilgraf R, et al. Inhibition of protein kinase CK2 expression and activity blocks tumor cell growth. Mol Cell Biochem. 2010; 333:159–67. [PubMed: 19629644]
27. Hamacher R, Saur D, Fritsch R, Reichert M, Schmid RM, Schneider G. Casein kinase II inhibition induces apoptosis in pancreatic cancer cells. Oncol Rep. 2007; 18:695–701. [PubMed: 17671722]
28. Piazza FA, Ruzzene M, Gurrieri C, et al. Multiple myeloma cell survival relies on high activity of protein kinase CK2. Blood. 2006; 108:1698–707. [PubMed: 16684960]
29. Yde CW, Frogne T, Lykkesfeldt AE, Fichtner I, Issinger OG, Stenvang J. Induction of cell death in antiestrogen resistant human breast cancer cells by the protein kinase CK2 inhibitor DMAT. Cancer Lett. 2007; 256:229–37. [PubMed: 17629615]
30. Lawnicka H, Kowalewicz-Kulbat M, Sicinska P, Kazimierczuk Z, Grieb P, Stepien H. Anti-neoplastic effect of protein kinase CK2 inhibitor, 2-dimethylamino-4,5,6,7-tetrabromobenzimidazole (DMAT), on growth and hormonal activity of human adrenocortical carcinoma cell line (H295R) in vitro. Cell Tissue Res. 2010; 340:371–9. [PubMed: 20383646]
31. Ruzzene M, Penzo D, Pinna LA. Protein kinase CK2 inhibitor 4,5,6,7-tetrabromobenzotriazole (TBB) induces apoptosis and caspase-dependent degradation of haematopoietic lineage cell-specific protein 1 (HS1) in Jurkat cells. Biochem J. 2002; 364:41–7. [PubMed: 11988074]
32. Pagano MA, Meggio F, Ruzzene M, Andrzejewska M, Kazimierczuk Z, Pinna LA. 2-Dimethylamino-4,5,6,7-tetrabromo-1H-benzimidazole: a novel powerful and selective inhibitor of protein kinase CK2. Biochem Biophys Res Commun. 2004; 321:1040–4. [PubMed: 15358133]
33. Prudent R, Moucadel V, Lopez-Ramos M, et al. Expanding the chemical diversity of CK2 inhibitors. Mol Cell Biochem. 2008; 316:71–85. [PubMed: 18563535]
34. Gianoncelli A, Cozza G, Orzeszko A, Meggio F, Kazimierczuk Z, Pinna LA. Tetraiodobenzimidazoles are potent inhibitors of protein kinase CK2. BioorgMedicinal Chem. 2009; 17:7281–9.
35. Lopez-Ramos M, Prudent R, Moucadel V, et al. New potent dual inhibitors of CK2 and Pim kinases: discovery and structural insights. FASEB J. 2010; 24:3171–85. [PubMed: 20400536]
36. Siddiqui-Jain A, Drygin D, Streiner N, et al. CX-4945, an Orally Bioavailable Selective Inhibitor of Protein Kinase CK2, Inhibits Prosurvival and Angiogenic Signaling and Exhibits Antitumor Efficacy. Cancer Res. 2010; 70:10288–98. [PubMed: 21159648]
37. Kramerov AA, Saghizadeh M, Pan H, et al. Expression of protein kinase CK2 in astroglial cells of normal and neovascularized retina. Am J Pathol. 2006; 168:1722–36. [PubMed: 16651637]

38. Kramerov A, Saghizadeh M, Caballero S, et al. Inhibition of protein kinase CK2 suppresses angiogenesis and hematopoietic stem cell recruitment to retinal neovascularization sites. Mol Cell Biochem. 2008; 316:177–86. [PubMed: 18612802]
39. Sass G, Klinger N, Sirma H, et al. Inhibition of experimental HCC growth in mice by use of the kinase inhibitor DMAT. Intl J Oncol. 2011; 39:433–42.
40. Pierre F, Chua PC, O'Brien SE, et al. Pre-clinical characterization of CX-4945, a potent and selective small molecule inhibitor of CK2 for the treatment of cancer. Mol Cell Biochem. 2011; 356:37–43. [PubMed: 21755459]
41. Prudent R, Moucadel V, Nguyen C-H, et al. Antitumor Activity of Pyridocarbazole and Benzopyridoindole Derivatives that Inhibit Protein Kinase CK2. Cancer Res. 2010; 70:9865–74. [PubMed: 21118972]
42. Zheng Y, McFarland BC, Drygin D, et al. Targeting protein kinase CK2 suppresses prosurvival signaling pathways and growth of glioblastoma. Clin Cancer Res. 2013; 19:6484–94. [PubMed: 24036851]
43. Wang G, Ahmad KA, Ahmed K. Role of protein kinase CK2 in the regulation of tumor necrosis factor-related apoptosis inducing ligand-induced apoptosis in prostate cancer cells. Cancer Res. 2006; 66:2242–9. [PubMed: 16489027]
44. Trembley JH, Unger GM, Korman VL, et al. Nanoencapsulated anti-CK2 small molecule drug or siRNA specifically targets malignant cancer but not benign cells. Cancer Lett. 2012; 315:48–58. [PubMed: 22050909]
45. Fattal E, Barratt G. Nanotechnologies and controlled release systems for the delivery of antisense oligonucleotides and small interfering RNA. Br J Pharmacol. 2009; 157:179–94. [PubMed: 19366348]
46. Aukhil I, Joshi P, Yan Y, Erickson HP. Cell- and heparin-binding domains of the hexabrachion arm identified by tenascin expression proteins. J Biol Chem. 1993; 268:2542–53. [PubMed: 7679097]
47. Brown MS, Diallo OT, Hu M, et al. CK2 Modulation of NF-κB, TP53, and the Malignant Phenotype in Head and Neck Cancer by Anti-CK2 Oligonucleotides In vitro or In vivo via Sub–50-nm Nanocapsules. Clin Cancer Res. 2010; 16:2295–307. [PubMed: 20371694]
48. Trembley JH, Unger GM, Korman VL, et al. Tenfibgen ligand nanoencapsulation delivers bi-functional anti-CK2 RNAi oligomer to key sites for prostate cancer targeting. PLoS One. 201410.1371/journal.pone.0109970
49. Unger GM, Kren BT, Korman VL, et al. Mechanism and efficacy of sub-50 nm tenfibgen nanocapsules for cancer cell-directed delivery of anti-CK2 RNAi to primary and metastatic squamous cell carcinoma. Molec Cancer Ther. 2014; 13:2018–29. [PubMed: 24867250]
50. Slaton JW, Unger GM, Sloper DT, Davis AT, Ahmed K. Induction of apoptosis by antisense CK2 in human prostate cancer xenograft model. Mol Cancer Res. 2004; 2:712–21. [PubMed: 15634760]
51. Pettaway CA, Pathak S, Greene G, et al. Selection of highly metastatic variants of different human prostatic carcinomas using orthotopic implantation in nude mice. Clin Cancer Res. 1996; 2:1627–36. [PubMed: 9816342]
52. Pagano MA, Andrzejewska M, Ruzzene M, et al. Optimization of protein kinase CK2 inhibitors derived from 4,5,6,7-tetrabromobenzimidazole. J Med Chem. 2004; 47:6239–47. [PubMed: 15566294]
53. Trembley JH, Unger GM, Tobolt DK, et al. Systemic administration of antisense oligonucleotides simultaneously targeting CK2alpha and alpha' subunits reduces orthotopic xenograft prostate tumors in mice. Mol Cell Biochem. 2011; 356:21–35. [PubMed: 21761204]
54. Tuominen VJ, Ruotoistenmaki S, Viitanen A, Jumppanen M, Isola J. ImmunoRatio: a publicly available web application for quantitative image analysis of estrogen receptor (ER), progesterone receptor (PR), and Ki-67. Breast Cancer Res. 2010; 12:R56. [PubMed: 20663194]
55. Pinna LA, Allende JE. Protein kinase CK2 in health and disease: Protein kinase CK2: an ugly duckling in the kinome pond. Cell Mol Life Sci. 2009; 66:1795–9. [PubMed: 19387554]

56. Perea SE, Reyes O, Baladron I, et al. CIGB-300, a novel proapoptotic peptide that impairs the CK2 phosphorylation and exhibits anticancer properties both in vitro and in vivo. Mol Cell Biochem. 2008; 316:163–7. [PubMed: 18575815]
57. Gravina GL, Marampon F, Di Staso M, et al. 5-Azacitidine restores and amplifies the bicalutamide response on preclinical models of androgen receptor expressing or deficient prostate tumors. Prostate. 2010; 70:1166–78. [PubMed: 20333699]
58. Karantanos T, Corn PG, Thompson TC. Prostate cancer progression after androgen deprivation therapy: mechanisms of castrate resistance and novel therapeutic approaches. Oncogene. 2013; 32:5501–11. [PubMed: 23752182]
59. Schrecengost R, Knudsen KE. Molecular pathogenesis and progression of prostate cancer. Semin Oncol. 2013; 40:244–58. [PubMed: 23806491]
60. Lin D, Gout PW, Wang Y. Lessons from in-vivo models of castration-resistant prostate cancer. Curr Opin Urol. 2013; 23:214–9. [PubMed: 23385975]
61. Nelson EC, Cambio AJ, Yang JC, Ok JH, Lara PN Jr, Evans CP. Clinical implications of neuroendocrine differentiation in prostate cancer. Prostate Cancer Prostatic Dis. 2007; 10:6–14. [PubMed: 17075603]
62. Bluemn EG, Nelson PS. The androgen/androgen receptor axis in prostate cancer. Curr Opin Oncol. 2012; 24:251–7. [PubMed: 22327838]
63. Tzelepi V, Zhang J, Lu JF, et al. Modeling a lethal prostate cancer variant with small-cell carcinoma features. Clin Cancer Res. 2012; 18:666–77. [PubMed: 22156612]
64. Anbazhagan R, Sakakura T, Gusterson BA. The distribution of immunoreactive tenascin in the epithelial-mesenchymal junctional areas of benign and malignant squamous epithelia. Virchows Arch B Cell Pathol Incl Mol Pathol. 1990; 59:59–63. [PubMed: 1696042]
65. Erickson HP, Bourdon MA. Tenascin: an extracellular matrix protein prominent in specialized embryonic tissues and tumors. Annu Rev Cell Biol. 1989; 5:71–92. [PubMed: 2480799]
66. Tuxhorn JA, Ayala GE, Rowley DR. Reactive stroma in prostate cancer progression. J Urol. 2001; 166:2472–83. [PubMed: 11696814]
67. Tomas D, Ulamec M, Hudolin T, Bulimbasic S, Belicza M, Kruslin B. Myofibroblastic stromal reaction and expression of tenascin-C and laminin in prostate adenocarcinoma. Prostate Cancer Prostatic Dis. 2006; 9:414–9. [PubMed: 16652121]
68. Zagzag D, Shiff B, Jallo GI, et al. Tenascin-C promotes microvascular cell migration and phosphorylation of focal adhesion kinase. Cancer Res. 2002; 62:2660–8. [PubMed: 11980665]
69. Schenk S, Chiquet-Ehrismann R, Battegay EJ. The fibrinogen globe of tenascin-C promotes basic fibroblast growth factor-induced endothelial cell elongation. Mol Biol Cell. 1999; 10:2933–43. [PubMed: 10473637]
70. Oskarsson T, Acharyya S, Zhang XH, et al. Breast cancer cells produce tenascin C as a metastatic niche component to colonize the lungs. Nat Med. 2011; 17:867–74. [PubMed: 21706029]
71. Yokoyama K, Erickson HP, Ikeda Y, Takada Y. Identification of amino acid sequences in fibrinogen gamma-chain and tenascin C C-terminal domains critical for binding to integrin alpha vbeta 3. J Biol Chem. 2000; 275:16891–8. [PubMed: 10747940]
72. Carver LA, Schnitzer JE. Caveolae: mining little caves for new cancer targets. Nat Rev Cancer. 2003; 3:571–81. [PubMed: 12894245]
73. Lupp S, Gumhold C, Ampofo E, Montenarh M, Rother K. CK2 kinase activity but not its binding to CK2 promoter regions is implicated in the regulation of CK2alpha and CK2beta gene expressions. Mol Cell Biochem. 2013; 384:71–82. [PubMed: 23963994]
74. Calabrese EJ. Hormesis and medicine. Br J Clin Pharmacol. 2008; 66:594–617. [PubMed: 18662293]
75. Zheng Y, McFarland BC, Drygin D, et al. Targeting Protein Kinase CK2 Suppresses Pro-survival Signaling Pathways and Growth of Glioblastoma. Clin Cancer Res. 2013
76. Prudent R, Moucadel V, Nguyen CH, et al. Antitumor activity of pyridocarbazole and benzopyridoindole derivatives that inhibit protein kinase CK2. Cancer Res. 2010; 70:9865–74. [PubMed: 21118972]

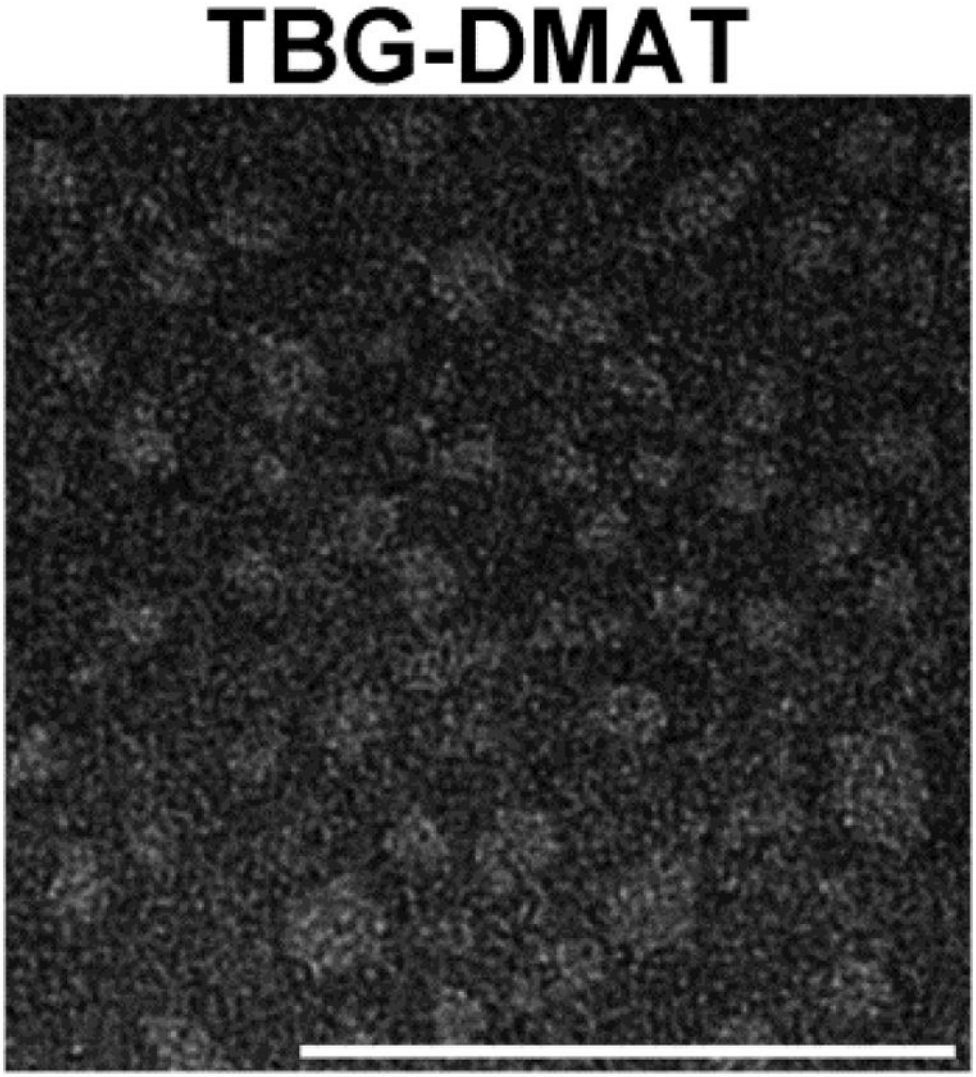

Figure 1.
Transmission electron micrograph of TBG-DMAT nanocapsules for *in vivo* studies. Scale bar is 100 nm.

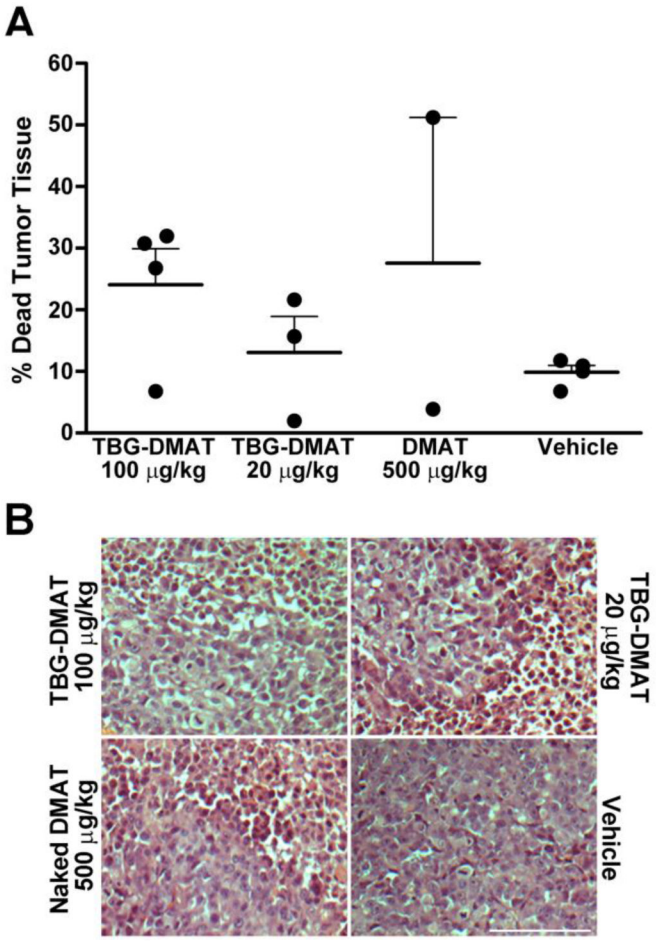

Figure 2. Effect of TBG-DMAT compared with DMAT on xenograft prostate tumors

(**A)** Effect on xenograft tumor mass following treatment with TBG-DMAT or DMAT. Tumor tissue from PC3-LN4 xenografts was excised following treatment with vehicle (control), DMAT and TBG-DMAT. The tumors were weighed before and after removal of dead liquefied tissue, and the percent change in tumor mass was calculated. Means are presented and error bars represent SE. (**B**) Representative H&E staining of tumors following treatment of tumor bearing mice with TBG-DMAT, naked DMAT and vehicle. Scale bar is 100 μm.

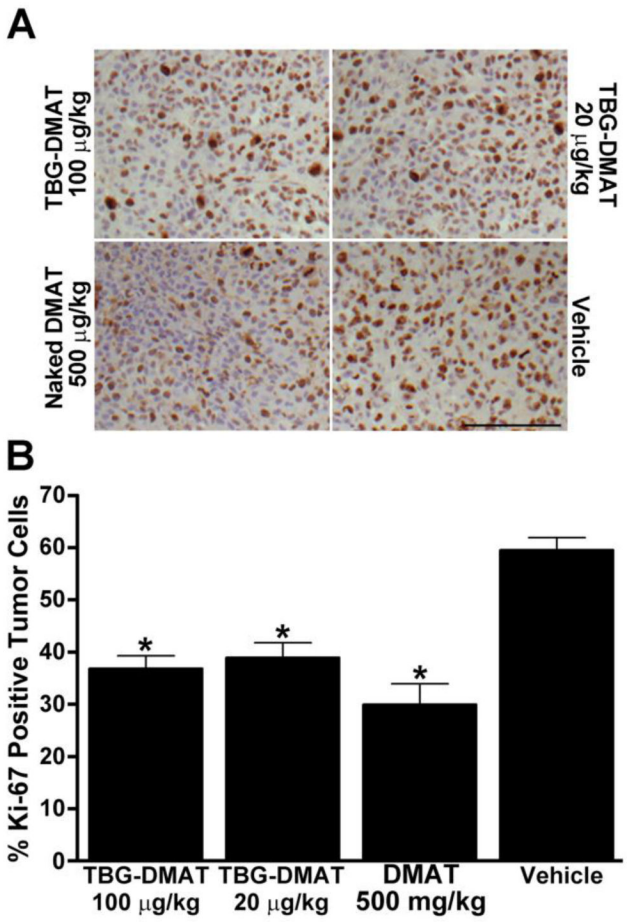

Figure 3. Analysis of Ki-67 expression in tumors following *in vivo* treatment with vehicle (control), DMAT and TBG-DMAT

(**A)** Formalin fixed and paraffin embedded tumors were processed for Ki-67 immunohistochemistry. Representative pictures are shown. Scale bar is 100 μm. (**B)** The percent of Ki-67 positive cells was analyzed as described in Materials and Methods and is shown graphically. Least-Squares means are presented and error bars represent SE. * $p < 0.002$ relative to vehicle.

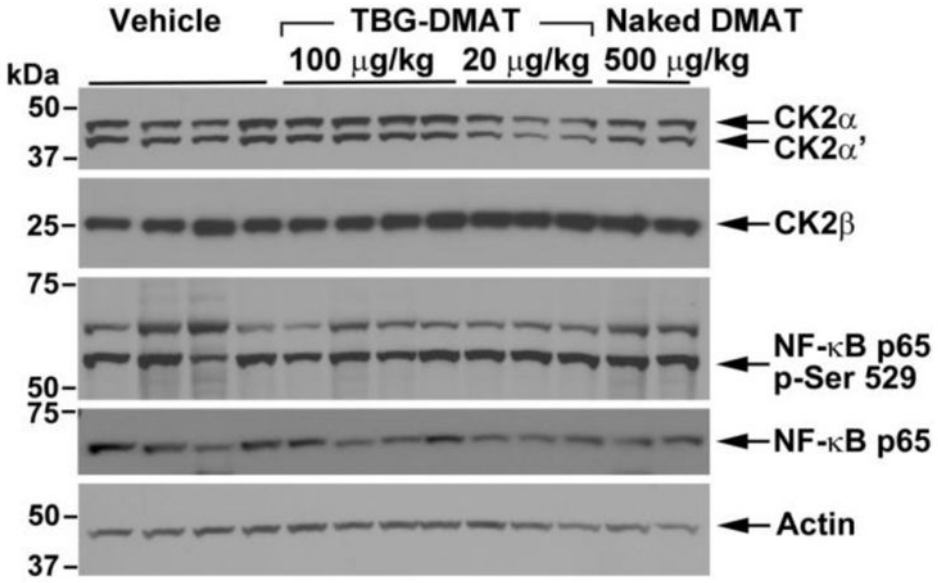

Figure 4. Immunoblot analysis of whole cell lysates from TBG-DMAT, naked DMAT and vehicle treated PC3-LN4 xenograft tumors

Whole cell lysates were prepared from the tumors and subjected to SDS polyacrylamide gel electrophoresis and immunoblot analysis with various antibodies as shown. Actin expression was used to control for protein loading. The proteins detected and molecular weight markers are shown on the right and left, respectively. Quantitation was performed using ImageJ and the data normalized to actin expression is presented in Table 2.

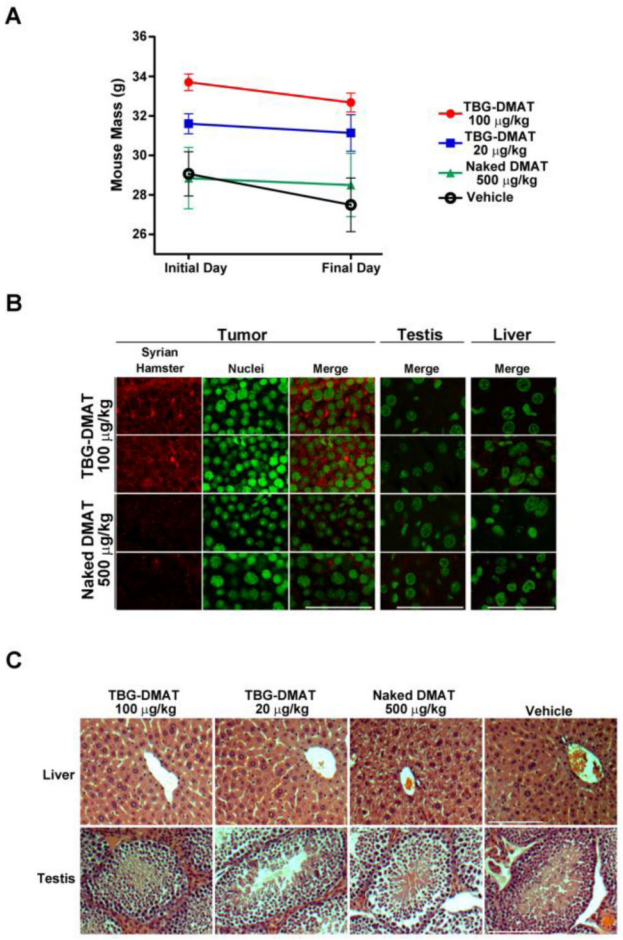

Figure 5. Lack of effects of TBG-DMAT treatment on mouse weight and organs and specific detection of TBG-DMAT in tumor

(A) The mass of the mice on the initial treatment day and the final sacrifice day is graphed for each treatment group. Means are presented and error bars represent SE. **(B)** Detection of TBG-DMAT in tumor but not testis or liver. Tissue sections from mice treated with 100 μg/kg TBG-DMAT or 500 μg/kg naked DMAT were subjected to immunofluorescence analysis for Syrian hamster IgG. Nuclei were counterstained with Sytox® Green. Scale bar is 100 μm. **(C)** Representative H&E staining of liver and testis following treatment of tumor bearing mice with TBG-DMAT, naked DMAT and vehicle. Scale bar is 100 μm.

Table 1

Nanocapsule Characteristics and Information

Shell Ligand	Particle Size (nm)[1]	Zeta Potential (meV)[2]	Morphology[3]	Cargo
Tenfibgen (TBG) 27 kDa[4]	14.6 ± 1.2	−8.6 ± 2.2	Uniform, Single Capsules	DMAT

[1] Mean ± SEM of the average elliptical diameter determined from AFM micrographs of 25 capsules from two different preparations after drying on mica at 0.5 ng/ml.

[2] Average surface charge measured by DLS across a 20 volt potential in 1 mM KCl at 2 μg/ml. Data shown are the mean ± SE of 15 independent measurements.

[3] Morphology of all nanocapsules determined by visual AFM observation as uniform, single capsules.

[4] Calculated and Laemmli SDS-PAGE-determined apparent molecular mass.

Table 2

Immunoblot Expression Levels in DMAT Treated PC3-LN4 Tumors[1]

Protein Analyzed	TBG-DMAT 100 μg/kg[2] N=4	TBG-DMAT 20 μg/kg[3] N=3	Naked DMAT 500 μg/kg[4] N=2	Vehicle[5] N=4
CK2α	1.01 ± 0.05 (p = 0.997)	0.59 ± 0.08 (p = 0.004)	1.03 ± 0.17 (p = 0.989)	1
CK2α′	0.92 ± 0.07 (p = 0.653)	0.44 ± 0.07 (p = 0.0004)	0.91 ± 0.13 (p = 0.697)	1
CK2β	0.92 ± 0.08 (p = 0.944)	1.40 ± 0.84 (p = 0.167)	0.89 ± 0.005 (p = 0.930)	1
NF-κB p65	0.71 ± 0.10 (p = 0.074)	0.59 ± 0.10 (p = 0.023)	0.87 ± 0.17 (p = 0.712)	1
NF-κB p65 p-Ser529	0.82 ± 0.06 (p = 0.215)	1.02 ± 0.09 (p = 0.997)	1.41 ± 0.19 (p = 0.017)	1

[1] All values normalized to actin expression and expressed relative to vehicle control treatment as mean ± SE. p values are listed underneath the corresponding protein expression value for comparison with vehicle control.

[2] Administered once daily, first 2 doses iv, last 6 doses ip, all doses at 100 μg/kg.

[3] Administered once daily, first 2 doses iv at 100 μg/kg, last 4 doses ip at 20 μg/kg.

[4] Administered once daily, all 6 doses ip at 500 μg/kg.

[5] Administered once daily, all 8 doses ip.